JACS
JOURNAL OF THE AMERICAN CHEMICAL SOCIETY
Article
pubs.acs.org/JACS

Dialkoxybithiazole: A New Building Block for Head-to-Head Polymer Semiconductors

Xugang Guo,[†,‡] Jordan Quinn,[§] Zhihua Chen,[§] Hakan Usta,[§] Yan Zheng,[§] Yu Xia,[§] Jonathan W. Hennek,[†] Rocío Ponce Ortiz,[†,∥] Tobin J. Marks,*[,†] and Antonio Facchetti*[,†,§]

[†]Department of Chemistry and the Materials Research Center, Northwestern University, 2145 Sheridan Road, Evanston, Illinois 60208, United States

[‡]Department of Chemistry, South University of Science and Technology of China, No. 1088, Xueyuan Boulevard, Shenzhen, Guangdong 518055, China

[§]Polyera Corporation, 8045 Lamon Avenue, Skokie, Illinois 60077, United States

[∥]Department of Physical Chemistry, University of Málaga, Campus de Teatinos s/n, Málaga 29071, Spain

Supporting Information

ABSTRACT: Polymer semiconductors have received great attention for organic electronics due to the low fabrication cost offered by solution-based printing techniques. To enable the desired solubility/processability and carrier mobility, polymers are functionalized with hydrocarbon chains by strategically manipulating the alkylation patterns. Note that head-to-head (HH) linkages have traditionally been avoided because the induced backbone torsion leads to poor $\pi-\pi$ overlap and amorphous film microstructures, and hence to low carrier mobilities. We report here the synthesis of a new building block for HH linkages, 4,4′-dialkoxy-5,5′-bithiazole (**BTzOR**), and its incorporation into polymers for high performance organic thin-film transistors. The small oxygen van der Waals radius and intramolecular S(thiazolyl)···O(alkoxy) attraction promote HH macromolecular architectures with extensive π-conjugation, low bandgaps (1.40−1.63 eV), and high crystallinity. In comparison to previously reported 3,3′-dialkoxy-2,2′-bithiophene (**BTOR**), **BTzOR** is a promising building block in view of thiazole geometric and electronic properties: (a) replacing (thiophene)C−H with (thiazole)N reduces steric encumbrance in **−BTzOR−Ar−** dyads by eliminating repulsive C−H···H−C interactions with neighboring arene units, thereby enhancing $\pi-\pi$ overlap and film crystallinity; and (b) thiazole electron-deficiency compensates alkoxy electron-donating characteristics, thereby lowering the **BTzOR** polymer HOMO versus that of the **BTOR** analogues. Thus, the new **BTzOR** polymers show substantial hole mobilities (0.06−0.25 $cm^2/(V\,s)$) in organic thin-film transistors, as well as enhanced I_{on}:I_{off} ratios and greater ambient stability than the **BTOR** analogues. These geometric and electronic properties make **BTzOR** a promising building block for new classes of polymer semiconductors, and the synthetic route to **BTzOR** reported here should be adaptable to many other bithiazole-based building blocks.

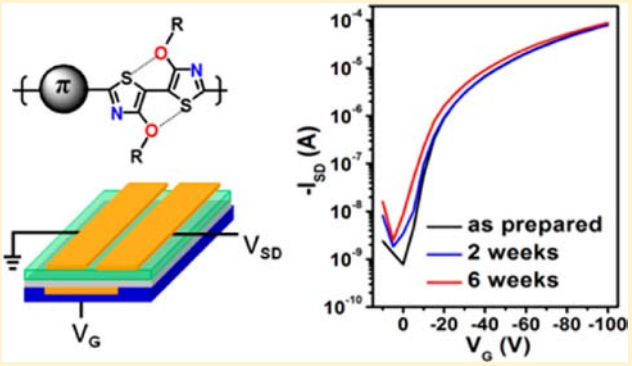

INTRODUCTION

Polymeric semiconductors are important materials classes both for fundamental soft matter charge transport studies and for flexible opto-electronics technologies.[1−8] In both areas, optimum materials should possess good solubility/processability, tunable bandgaps, tailorable frontier molecular orbital (FMO) energies, and optimally ordered film microstructure and morphology[9−16] to achieve high carrier mobility in organic thin-film transistors (OTFTs),[1,3] and sizable power conversion efficiencies in organic photovoltaic cells (OPVs),[4] combined with acceptable environmental stability.[5] To increase polymer processability, a common strategy is to functionalize the backbone with solubilizing groups (Figure 1a),[17,18] commonly alkyl chains (R). However, depending on the substitution regiochemistry, this tactic can negatively affect core electronic structure and solid-state packing, hence device performance. For example, the substituent steric repulsions engendered in head-to-head (HH) π-monomer linkages typically induce backbone twisting and greatly reduced π-conjugation as in regioirregular poly(3-alkylthiophene)s (Figure 1b).[6]

Several strategies have been employed to access highly conjugated, high-performance semiconducting polymers. First, efficient synthetic routes have been developed to achieve self-oriented head-to-tail poly(3-alkylthiophene)s having regioregular alkyl chain placement (Figures 1c and 2a);[19,20] the resulting highly regioregular poly(3-hexylthiophene) (rr-P3HT) is highly conjugated and with a mobility >0.1 $cm^2/(V$

Received: December 10, 2012
Published: January 17, 2013

dx.doi.org/10.1021/ja3120532 | J. Am. Chem. Soc. 2013, 135, 1986−1996

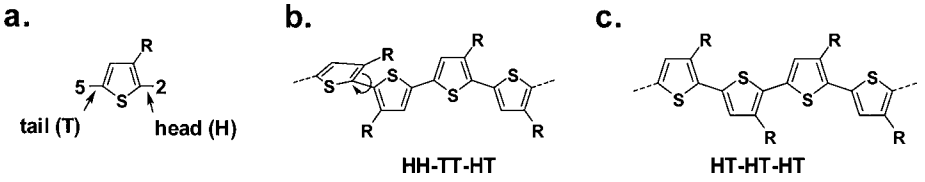

Figure 1. Chemical structures of (a) 3-alkylthiophene, in which the 2-position is designated head (H) and the 5-position is designated tail (T); (b) regioirregular poly(3-alkylthiophene), which contains head-to-head (HH), tail-to-tail (TT), and head-to-tail (HT) linkages; and (c) regioregular poly(3-alkylthiophene), which contains exclusively head-to-tail (HT) linkages.

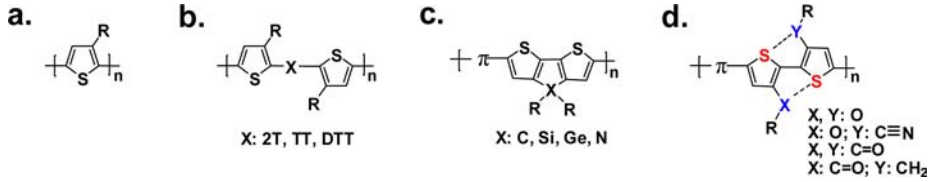

Figure 2. Design strategies for polymer semiconductors to achieve enhanced planarity, conjugation, and mobility by introducing: (a) Substituent regioregularity. (b) Spacer groups (X): 2T = bithiophene; TT = thienothiophene; DTT = dithienothiophene or other thiophene/thiazole-terminated groups. (c) Linker atoms (X) for conformational locking. (d) Head-to-head linkages via intramolecular S···O conformational locking; S···O = S(thienyl)···O(alkoxy) and S(thienyl)···O(carbonyl).

s) (a record at the time for a polymer TFT).[21] Nevertheless, the limited chemical structure variability leads to limited diversity and opto-electronic properties for poly(3-alkylthiophene)s. Subsequently, Ong and McCulloch reported polythiophenes, PQT[22] and PBTTT,[23] respectively, with thiophene-arene spacers to yield p-type polymers with 3-D lamellar structures and substantial hole mobility (0.1−0.6 $cm^2/(V\ s)$).[3,24] This pioneering strategy of using thiophene-arene spacers (Figure 2b) has been now widely adopted for materials design. The principal limitations of this approach are polymer solubility[25,26] because the spacers are typically nonalkylated arenes, such as bithiophene (2T),[22] thienothiophene (TT),[23,27] and dithienothiophene(DTT),[28] and the requirement that the spacer be thiophene/thiazole-terminated arenes, such as naphthodithiophene (NDT)[26] and thiazolothiazole (TzTz),[29] and benzobisthiazole (BBTz).[30] Bulkier arene-terminated spacers, such as indenofluorene[31] and benzothienobenzothiophene,[26] likely induce high degrees of polymer backbone torsion and destroy $\pi-\pi$ stacking; therefore, the OTFTs fabricated from such polymers exhibit low TFT mobilities[31] or are TFT inactive.[32] Another successful approach uses linker atoms such as C, Si, Ge, and N to lock the polymer backbone conformation (Figure 2c). Thus, cyclopentadithiophene,[33,34] dithienosilole/germole,[35−37] and dithienopyrrole[38] incorporation promote main-chain coplanarity along with improved processability. The limitation here is that the out-of-plane disposition of the linker substituents may interfere with $\pi-\pi$ stacking[36,39] and/or reduce solubility due to the extended fused architecture.[38] Although the linker atom strategy yields polymers having extended conjugation and small bandgaps, it generally leads to moderate mobility $<10^{-2}$ $cm^2/(V\ s)$[35,40] due to enlarged $\pi-\pi$ stacking[34] and/or limited side chain interdigitation. This linker atom strategy has been highly successful for designing low-bandgap polymer OPV materials, for which mobilities of $10^{-3}-10^{-2}$ $cm^2/(V\ s)$ are usually sufficient. Also note that ultrahigh hole TFT mobilities up to 3 $cm^2/(V\ s)$ have been achieved in benzothiadiazole-cyclopentadithiophene copolymers; however, slow film deposition techniques such as drop-casting[34,41] or dip-coating[42] are usually required to achieve long-range microstructural order.[43]

In contrast to the above strategies, if HH linkage-based polymers could be constructed with coplanar backbone conformations, two intriguing characteristics should be possible: (a) alkyl substituents along with rotational freedom within the HH monomers should promote good solubility/processability; (b) the HH building block should be suitable for polymerization reactions with many arene classes, not only thiophene/thiazole-terminated derivatives, but also phenyl-terminated arenes due to HH substituent orientations, which should reduce steric congestion with neighboring arenes. Nevertheless, HH linkages have traditionally been avoided in polymer semiconductor design for alkyl substituents[6] because the van der Waals radius of the alkyl substituent methylene groups (2.0 Å)[44] typically imposes unacceptable steric hindrance, resulting in backbone torsion (Figure 1b). However, if the substituents have smaller van de Waals radii and/or engage in intramolecular noncovalent planarizing interactions (e.g., Figure 2d), the macromolecular conformation may approach coplanarity, even in the presence of HH linkages. In comparison to methylene groups, the oxygen van der Waals radius (1.4 Å) is far smaller, so that inserting an oxygen atom between the thienyl and methylene groups, combined with attractive S(thienyl)···O(alkoxy) interactions,[45,46] yields 3,3′-dialkoxy-2,2′-bithiophene (**BTOR**, Figures 3c), with a high degree of backbone coplanarity.[47] Furthermore, **BTOR**-based polymers yield excellent p-type (0.2 $cm^2/(V\ s)$)[48] or ambipolar transport.[49,50] Unfortunately, the very electron-rich character of **BTOR** strongly destabilizes the HOMO energies of the resulting polymers, limiting OTFT I_{on}:I_{off} ratios and likely long-term environmental stability. Also note that a significant S···O interaction exists in the S(thienyl)···O(carbonyl) derivatives (Figure 2d),[51] in which the carbonyl group is electron-withdrawing. The S···O-induced backbone coplanarity, TPD electron-deficiency, and high alkyl chain density afford superior performance in both OTFTs[52] and OPVs.[53−55] This TPD versatility[56] highlights the importance of realizing new building blocks, which can simultaneously achieve significant backbone planarity, high solubilizing group densities, and desirable electronic properties.

In this regard, thiazole is an electron-deficient heterocycle,[57−59] and thiazole-based polymers exhibit, versus their

dx.doi.org/10.1021/ja3120532 | J. Am. Chem. Soc. 2013, 135, 1986−1996

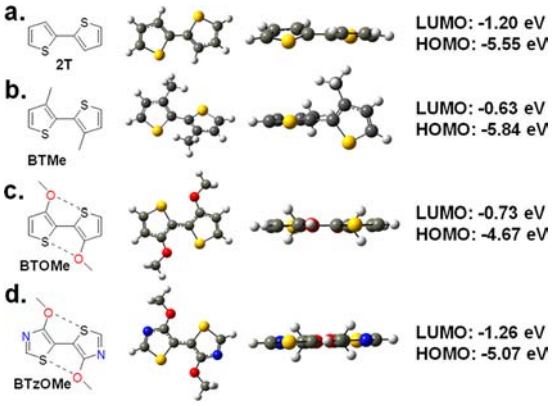

Figure 3. Chemical structures, optimized geometries, LUMO energies, and HOMO energies for (a) bithiophene (**2T**), (b) 3,3′-dimethyl-2,2′-bithiophene (**BTMe**), (c) 3,3′-dimethoxy-2,2′-bithiophene (**BTOMe**), and (d) 4,4′-dimethoxy-5,5′-bithiazole (**BTzOMe**). Calculations were carried out at the DFT//B3LYP/6-31G** level.

thiophene analogues, lower-lying HOMOs and greater TFT air stability.[60−62] In the present context, thiazole should reduce steric congestion-induced backbone twisting by eliminating repulsive C−H···H−C interactions when linked to arene counits.[63−65] However, thiazole-based small molecules and polymers typically exhibit lower hole mobilities than the corresponding thiophene analogues due to nonoptimal HOMO energetics as well as synthetic barriers to accessing high molecular weights.[62,66] We hypothesized that combining electron-poor thiazoles with the electron-donating alkoxy substituents would balance the electronic structure such that hole mobility would be enhanced while retaining low-HOMO characteristics such as air stability and large current on−off ratios. Comparative geometries and DFT-derived frontier MO energies are shown in Figure 3 for 2,2′-bithiophene (**2T**), 3,3′-dimethyl-2,2′-bithiophene (**BTMe**), 3,3′-dimethoxy-2,2′-bithiophene (**BTOMe**), and 4,4′-dimethoxy-5,5′-bithiazole (**BTzOMe**). Methoxy group incorporation leads to coplanar geometries for both **BTOMe** and **BTzOMe** (dihedral angle ∼0°) versus twisted **2T** (∼22°) and **BTMe** (∼68°). Importantly, the **BTzOMe** HOMO (−5.07 eV) lies between that of **BTMe** (−5.84 eV) and that of **BTOMe** (−4.67 eV), with the **BTzOMe** LUMO being the lowest in the series, suggesting a promising candidate for soluble, environmentally stable, semiconducting π-conjugated polymers.

Scheme 1. Synthetic Route to BTzOR Monomers and BTzOR/BTOR-Based Polymers[a]

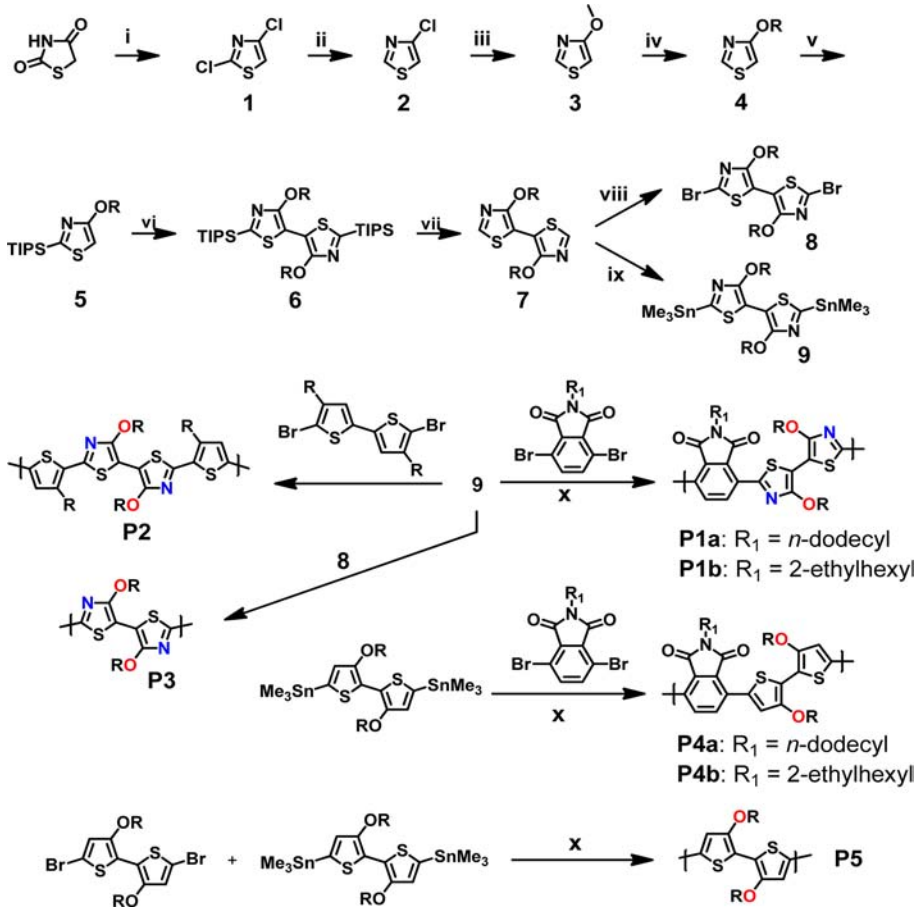

[a]R = *n*-dodecyl. Reagents/conditions: (i) $POCl_3$, C_6H_5N, reflux; (ii) Zn, HOAc, reflux; (iii) NaOMe, CuI, MeOH, reflux; (iv) PTSA, $C_{12}H_{25}OH$, toluene, 130 °C; (v) *n*-BuLi, THF, −78 °C, then room temperature; TIPSCl, −78 °C, then room temperature; (vi) *n*-BuLi, THF, −78 °C, then room temperature; $Fe(acac)_3$, 0 °C, then 80 °C; (vii) TBAF, THF, 0 °C, then room temperature; (viii) NBS, $CHCl_3$, 60 °C; (ix) *n*-BuLi, THF, −78 °C, then room temperature; Me_3SnCl, −78 °C, then 60 °C; (x) $Pd_2(dba)_3$, P(*o*-tolyl)$_3$, toluene.

dx.doi.org/10.1021/ja3120532 | *J. Am. Chem. Soc.* 2013, 135, 1986−1996

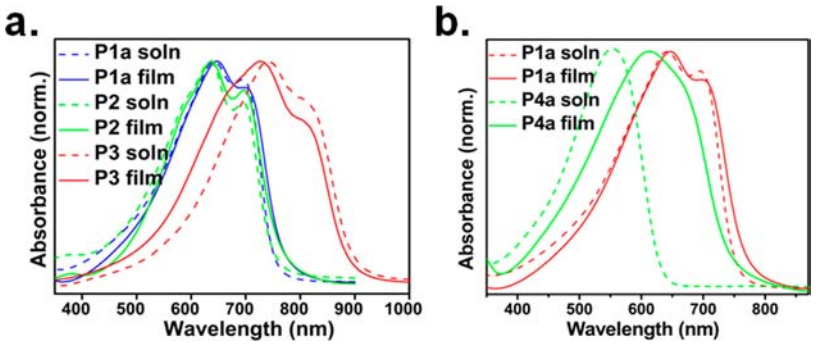

Figure 4. (a) Optical absorption spectra of **BTzOR**-based polymers in $CHCl_3$ solutions (dashed line, 1×10^{-5} M) and as thin films (solid line) cast from chloroform solution (5 mg/mL). (b) Optical absorption spectra of **BTzOR**-based polymer **P1a** and **BTOR**-based polymer analogue **P4a** in chloroform solution (dashed line, 1×10^{-5} M) and as pristine films (solid line) cast from chloroform solution (5 mg/mL).

Table 1. Physicochemical and Thin-Film Transistor Properties of Polymers P1−P5

polymer	M_n (kDa)	PDI	λ_{max} film (nm)	E_g^{opt} (eV)	HOMO (eV)	$T_{annealing}$ (°C)[a]	μ_h ($cm^2/(V\ s)$)[b]	I_{on}/I_{off}[b]
P1a	5.2	3.2	647	1.62	−5.18	210	0.06	10^5
P1b	34.6	3.7	668	1.58	−5.16	150	0.13	10^5
P2	11.7	2.0	637	1.63	−4.94	120	0.15 (0.25)[c]	10^3 (10^2)[c]
P3	8.8	5.2	727	1.40	−4.80	120	0.07[d] (0.15)[c]	10^{2d} (10^2)[c]
P4a	6.3	3.6	614	1.66	−5.07	150	0.07	10^4
P4b	44.3	2.8	618	1.66	−5.09	room temp	0.04	10^3
P5	9.0	4.2	644	1.64	−4.55	90	0.02[d]	<5[d]

[a]Annealing temperature, which yields optimal device performance. [b]BGTC OTFT performance measured in air. [c]TGBC OTFT performance measured in air. [d]Device measured in vacuum.

RESULTS AND DISCUSSION

In this Article, we report the synthesis of a novel dialkoxybithiazole (**BTzOR**) building block and its incorporation into polymer backbones for OTFT applications. The new series of **BTzOR**-based polymer semiconductors shows extensive conjugation, low optical bandgaps, and significant crystallinity; their implementation in OTFTs yields substantial hole mobilities (0.06−0.25 $cm^2/(V\ s)$), as well as significantly enhanced I_{on}:I_{off} ratios and ambient stability versus **BTOR**-based analogues. The solubilizing ability, as well as geometric and electronic properties, makes **BTzOR** a promising prototype building block for new classes of polymeric semiconductors.

Synthesis of BTzOR-Based Monomers and Polymers. The chemistry of thiazole differs significantly from that of thiophene,[67,68] making the synthesis of bithiazole-based building blocks far more challenging and less developed.[69−71] For example, 4,4′-dialkyl-2,2′-bithiazole, a tail-to-tail bithiazole unit, was prepared from halomethyl ketones and dithiooxamide,[70] which is greatly different from the synthesis of 4,4′-dialkyl-2,2′-bithiophene achieved via dimerization of alkylthiophenes.[72] Furthermore, when 2,5-dibromothiazole is reacted with 2,5-distannylated thiophenes, highly regioregular polymers with an estimated head-to-tail content >90% are achieved, which is not the case for polymerizations of 3-subsituted-2,5-dibromothiophenes.[73] Furthermore, as reported in the Introduction, thiazole-based organic semiconductors also show electrical properties and film microstructures distinctively different from those of the thiophene analogues. Head-to-head linkage in polythiophene strongly twists the polymer backbone resulting in amorphous or poorly crystalline films.[6] On the other hand, Curtis[70] and Yamamoto[74] found that the head-to-head bithiazole homopolymers achieve a high degree of polymer backbone coplanarity and extensive π-stacking in the solid state due to the reduced steric hindrance of thiazole versus thiophene. Despite the interesting chemistry and different solid-state properties, bithiazole-based copolymers are very rare due to the synthetic challenges.[61,70,71,75−77]

The synthetic routes to the key intermediate **BTzOC12** (**7**) and the corresponding polymers **P1−P3** are depicted in Scheme 1. First, 4-chlorothiazole (**2**)[78] is converted to 4-methoxythiazole (**3**) via a nucleophilic aromatic substitution.[47] Transetherification of **3** produces compound **4**,[47] which exhibits reactivity very different from that of the thiophene analogue, 3-dodecoxythiophene. The thiazole 2-position is the most reactive site,[79] rendering the synthetic strategy used for **BTOR**[47] not viable for **BTzOR**. Therefore, after protecting the 2-position of **4** with a triisopropylsilyl (TIPS) group, the 5-position is lithiated and subsequent Fe-mediated coupling[80] affords **BTzOC12** (**7**) in high yield (96%), which is then converted to the monomers **8** and **9**. **BTzOR**-based polymers **P1−P3**, as well as the corresponding **BTOR**-based polymer analogues **P4** and **P5** (vide infra), were synthesized using Stille coupling. The identity and purity of all polymers are supported by elemental analysis (EA) and high-temperature ^{1}H NMR spectra in 1,1,2,2-tetrachloroethane-d_2. As compared to previously reported **BTOR**-phthalimide copolymer **P4a** ($M_n \approx 200$ kDa),[48] **P1a** is obtained with significantly lower M_n for the soluble fraction (5.2 kDa), probably due to the reduced polymer solubility. The lower solubility of **P1a** is an indication of strong intra- and/or intermolecular interactions. Thus, to compare the performance of thiazole-based **P1a** to the thiophene analogue, polymer **P4a** with $M_n \approx 6$ kDa was synthesized by lowering the polymerization temperature. Interestingly, **P1b** having branched *N*-2-ethylhexyl imide substituents achieves good solubility and high M_n (~35 kDa), comparable to **P4b** synthesized under the same conditions (~44 kDa). The M_n's of **P2** and **P3** are 11.7 and 8.8 kDa with polydispersities of 2.0 and 5.2, respectively.

dx.doi.org/10.1021/ja3120532 | J. Am. Chem. Soc. 2013, 135, 1986−1996

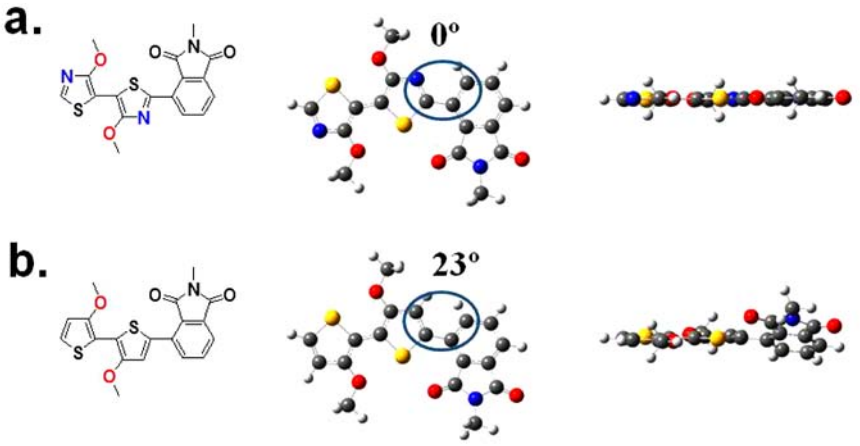

Figure 5. Optimized geometries for the polymer repeat units of (a) **P1** dialkoxybithiazole-phthalimide repeat unit, and (b) **P4** dialkoxybithiophene-phthalimide repeat unit. Calculations were carried out at the DFT//B3LYP/6-31G** level; dihedral angles between the planes of the donor and acceptor blocks and the regions of steric repulsion engendering torsion are indicated by blue circles. Alkyl substituents are replaced here by methyl groups to simplify the calculations.

Optical and Electrochemical Properties. Optical absorption spectra of the bithiazole polymers **P1**–**P3** in chloroform solutions and as thin films are shown in Figure 4a, and relevant data are collected in Table 1. All absorption profiles of the **BTzOR**-based polymers show a maximum (λ_{max}) in addition to an absorption shoulder, which is somewhat indicative of ordering.[24] The **BTzOR**-based polymers **P1**–**P3** exhibit extensive aggregation in solution as evidenced by the negligible blue-shift of the λ_{max} and the absorption shoulder on going from film to solution (<10 nm shift). These polymers exhibit large oscillator strengths in the visible, and the optical bandgaps (E_g^{opt}'s) estimated from the absorption edges of 1.62, 1.58, 1.63, and 1.40 eV for **P1a**, **P1b**, **P2**, and **P3**, respectively. Bulkier imide *N*-2-ethylhexyl groups usually result in slightly enlarged polymer bandgaps over linear imide substituents due to the increased intermolecular π–π stacking distance and attendant decreased π-orbital overlap.[55,81] Therefore, the smaller E_g^{opt} of **P1b** (1.58 eV) versus that of **P1a** (1.62 eV) is reasonably attributed to extended conjugation due to the higher **P1b** M_n, which also indicates that the **P1a** M_n is insufficient to reach saturation of the conjugation length. The narrow E_g^{opt}'s of the **BTzOR**-based polymers indicate extended polymer backbone conjugation, enabled by significant backbone coplanarity in **P2** and **P3**, as well as the electron-rich character of **BTzOR** in **P1**, albeit less than in **BTOR**. Figure 4b shows the optical spectra of phthalimide-**BTzOR** copolymer **P1a** and phthalimide-**BTOR** copolymer **P4a**; it is evident that replacing **BTOR** with **BTzOR** leads to smaller E_g^{opt}'s in the resulting polymers: 1.62 eV (**P1a**) vs 1.66 eV (**P4a**, Figure 4b), 1.58 eV (**P1b**) vs 1.66 eV (**P4b**, Figure S2), and 1.40 eV (**P3**) vs 1.64 eV (**P5**, Figure S3). The smaller E_g^{opt} of **P3** than that of **P5** is in good agreement with the calculated optical gaps of their repeating units (Figure 3c and d), which can be attributed to enhanced push–pull interactions in the alkoxythiazole unit of **P3**. Such push–pull interactions have been shown to be effective for lowering the optical gaps in small molecule chromophores.[82] Thus, as the polymer backbone expands, a very low bandgap (1.40 eV) is achieved in **P3**. Also, the replacement of **BTOR** with **BTzOR** results in structured absorption profiles for **P1** in solution as well as in the thin film state versus **P4**.[48] Because **BTzOR** is less electron-rich than **BTOR**, the smaller bandgap of **P1** must reflect the higher degree of backbone coplanarity versus **P4**, which also accounts for the structured absorption profiles and decreased solubility of **P1a**.

Next, DFT computation was carried out to clarify the electronic structures and optical properties of the **BTzOR**- and **BTOR**-based polymers. The energy-minimized dihedral angle (Figure 5) is ~23° between the phthalimide and alkoxythiophene planes,[83] while it is computed to be 0° between the phthalimide and alkoxythiazole planes. The greater coplanarity in the latter case is due to the elimination of repulsive C–H···H–C interactions[63,65] and the presence of S(thiazolyl)···O (carbonyl) interaction,[55] and therefore affords the smaller bandgaps and also structured absorption profiles. DFT calculation of the **P4** repeat unit yields a S(thiazolyl)···O (carbonyl) distance of 2.78 Å, which is significantly shorter than the sum of S and O van der Waals radius of 3.32 Å. The greater degrees of conformational coplanarity can be also expected in other **BTzOR**-based polymer semiconductors, making **BTzOR** units promising building blocks for developing highly conjugated heterocyclic polymer semiconductors.

The ionization potentials (IPs) of these polymers were next estimated using cyclic voltammetry (Figure 6), and the derived HOMO energies are compiled in Table 1. **P2** and **P3** have HOMOs at −4.94 and −4.80 eV, respectively, which are higher

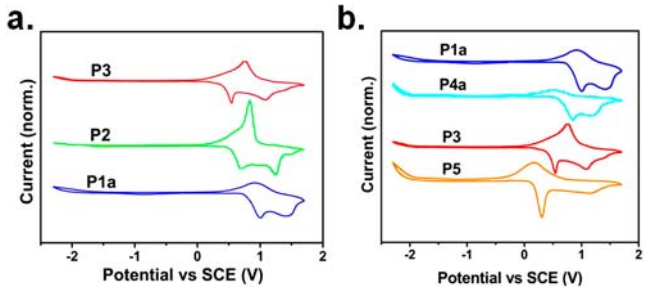

Figure 6. (a) Cyclic voltammograms of **BTzOR**-based polymers. (b) Comparison of cyclic voltammograms of **BTzOR**- and **BTOR**-based polymers. The measurements were carried out in 0.1 M $(n\text{-}Bu)_4N^+PF_6^-$ CH_3CN solution, and the Fc/Fc^+ redox couple was used as an external standard having an oxidation potential of +0.36 V vs SCE.

dx.doi.org/10.1021/ja3120532 | *J. Am. Chem. Soc.* 2013, 135, 1986–1996

than that of **P3HT** measured under identical conditions (−5.05 eV). The high HOMOs can lead to high off-currents and eroded device stability (vide infra).[6,38] By copolymerization with electron-deficient phthalimides,[84] polymers **P1a** and **P1b** achieve lower HOMOs of −5.16 eV to −5.18 eV. Importantly, replacement of **BTOR** with **BTzOR** lowers the HOMOs of **P1** and **P3** by ∼0.1 and ∼0.25 eV versus those of **P4** and **P5**, respectively (Table 1, Figure 6b), which indicates the less electron-rich characteristics of **BTzOR** versus **BTOR**. Note that replacing **BTOR** with **BTzOR** does not significantly lower the **P1** HOMO, which may reflect the higher degree of coplanarity in **P1**. While backbone torsion can lower the polymer HOMOs,[10,85] the eliminated C−H···H−C repulsive interactions in **P1** compress the bandgap, and the net result is that the HOMO is not significantly lower than in **P4**.

Thin-Film Transistor Response and Polymer Film Morphology. The charge transport properties of the new **BTzOR**-based polymers were investigated by fabricating bottom-gate/top-contact (BGTC) and top-gate/bottom-contact (TGBC) TFTs. For the BGTC devices, the polymers were dissolved in chloroform (10 mg/mL) at 50−60 °C on a hot plate, and then deposited by spin-coating the polymer solution under ambient conditions onto octadecyltrichlorosilane (OTS)-treated or hexamethyldisilazane (HMDS)-treated, p-doped Si (001) wafers having a 300 nm thermal SiO_2 dielectric layer. The spin-coating should be carried out within 5 min of polymer dissolution, because longer storage at room temperature leads to gelation of **P1a** and **P3**. After spin-coating, the polymer films were thermally annealed under vacuum over a range of temperatures (see the Supporting Information for details). Device characterization was performed under ambient or vacuum as specified. All of the present polymers exhibit distinct p-type response, and the optimal average performance data (at least five devices measured for each sample) are collected in Table 1. The average hole mobilities for **P1a**, **P1b**, **P2**, and **P3**-based BGTC OTFTs are 0.06, 0.13, 0.15, and 0.07 $cm^2/(V\ s)$ with current modulations (I_{on}/I_{off}) of 10^5, 10^5, 10^3, and 10^2 after thermally annealing at 210, 150, 120, and 120 °C, respectively. As for other organic TFTs, TGBC devices (see the Supporting Information for fabrication details) perform better,[86,87] for example, with average $\mu_h \approx 0.25\ cm^2/(V\ s)$ for **P2** TFT. The analysis of the TFT performance is instructive in understanding the difference between the **BTzOR**- and **BTOR**-based polymers. The progressive I_{on}/I_{off} fall from **P1** to **P3** nicely tracks the rise in the corresponding HOMO energies. Note that μ_h of **P4a** here (M_n = 6.3 kDa, μ_h = 0.07 $cm^2/(V\ s)$) is somewhat lower than that of high M_n **P4a** ($M_n \approx$ 200 kDa, μ_h = 0.17 $cm^2/(V\ s)$),[48] indicating that a substantial M_n is essential for optimum performance.[41,88,89] However, when a consistent comparison is carried out between thiazole polymers **P1b**/**P3** and thiophene analogues **P4b**/**P5**, the hole mobility of the thiazole family is up to ∼3× greater. For example, the average μ_h of **P1b** (M_n = 34.6 kDa) is 0.13 $cm^2/(V\ s)$, while the average μ_h of **P4b** (M_n = 44.3 kDa) is 0.04 $cm^2/(V\ s)$. The greater μ_h of the **BTzOR**-based polymer agrees with the higher degree of backbone coplanarity by eliminating C−H···H−C interactions (Figure 5) and/or greater film crystallinity (vide infra). Furthermore, the **BTzOR**-based OTFTs exhibit greater I_{on}/I_{off} values (>10−100×) and far greater I−V stability in ambient than the **BTOR**-based analogues (Figure 7). After 6 weeks in air, the mobility and I_{on}/I_{off} ratio of **P1a** OTFTs basically remain unchanged while the I_{on}/I_{off} ratio of **P4a** OTFTs falls by more than 100×, and the threshold voltage also drifts significantly for **P4a** OTFTs. These results are consistent with the more electron-deficient character of the thiazole core versus the thiophene core.

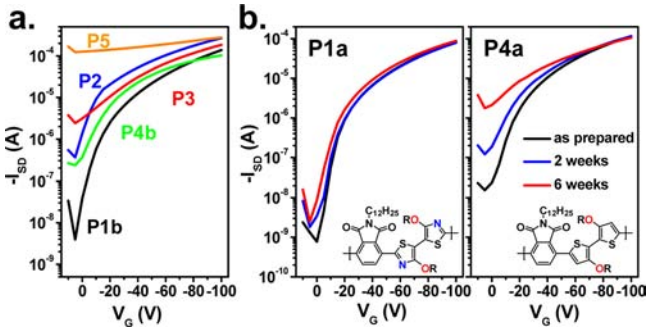

Figure 7. (a) Comparison of **P1**−**P5**-based OTFT transfer characteristics. (b) Comparison of transfer characteristics of **BTzOR**-based polymer **P1a** and **BTOR**-based **P4a** BGTC OTFTs stored and characterized in air.

To understand the charge transport properties of the new **BTzOR** head-to-head polymers, the film microstructures and morphologies were investigated by differential scanning calorimetry (DSC), specular X-ray diffraction (XRD), and atomic force microscopy (AFM). The DSC scan reveals no significant thermal transitions for the **BTzOC12**-based polymers in the range of 25−320 °C (Figure S1), similar to the **BTOR**-based analogues.[48] Figure 8 shows Θ−2Θ XRD scans and AFM topographic images of **P1** films, with those of **P4** films included for comparison. A single family of Bragg reflections assigned to the lamellar packing (lateral chain backbone to backbone distance) is observed for **P1a** and **P1b** films, with progressions up to the third order, indicating highly ordered film microstructures.[90] However, the **P4a** and **P4b** films show lower degrees of order and less intense lamellar diffraction features,[48] consistent with their featureless optical absorption spectra. The higher degree of ordering of **P1** (Figure 8) can be attributed to the higher degree of backbone coplanarity induced by deleting C−H···H−C repulsions

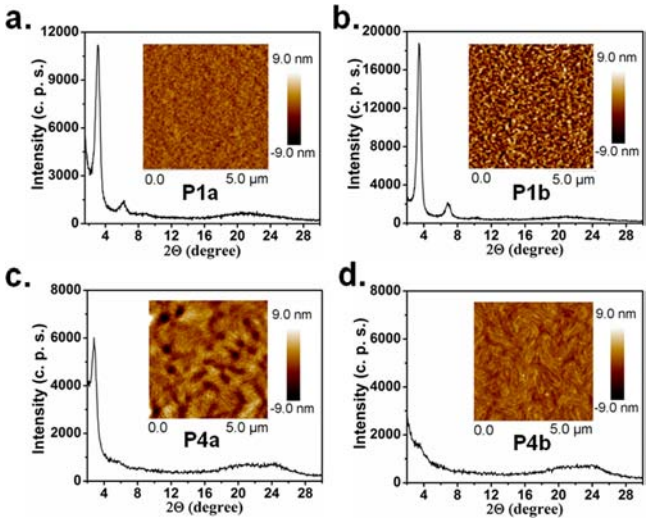

Figure 8. XRD scattering patterns and AFM data (inset: 5 × 5 μm topographic images) of **BTzOR**-based polymer **P1** and **BTOR**-based polymer **P4** films fabricated under conditions that yield the best-performing thin-film transistors.

dx.doi.org/10.1021/ja3120532 | J. Am. Chem. Soc. 2013, 135, 1986−1996

between the phthalimide and thiazole units (Figure 5), ultimately enhancing carrier mobility. Interestingly, the **BTzOR**-based polymer films do not exhibit any significant reflections from the polymer π-stacking in comparison to the weak π-stacking reflection (~24°) observed for the **BTOR**-based polymer **P4**[48] (note that the reflection at ~22° is due to the Si substrate). The absence of perpendicular π-stacking in **BTzOR**-based polymers and thus having a unique edge-on polymer backbone orientation[90] may also facilitate charge transport in **BTzOR** polymer OTFTs.[91] The thermal annealing-induced device performance enhancement corresponds well with the film microstructure evolution. For example, μ_h increases from 3.7×10^{-2} to 0.13 $cm^2/(V\ s)$ for a **P1b** TFT after thermally annealing at 150 °C. The XRD scans of the **P1b** films exhibit the strongest diffraction features after annealing at 150 °C versus those of films annealed at other temperatures. Note also that the AFM images show distinctively different **P1** and **P4** morphologies. **P4** has more textured and fibrillar-like domains and more distinct intergrain boundaries, which should act as charge carrier traps, while **P1** exhibits more extensive domain interconnectivity, which should enhance bulk charge transport.[38] The greater hole mobility of **P1b** versus **P1a** can be ascribed to the higher degree of film crystallinity as revealed by the XRD data (Figure 8a and b). The **P1b** films show more intense diffraction than the **P1a** films; hence, the greater crystallinity may be due to the higher M_n of **P1b**.[41,87]

CONCLUSIONS

We report an efficient synthetic route to the novel head-to-head polymer semiconductor building block, 4,4′-dialkoxy-5,5′-bithiazole (**BTzOR**), and the properties of the resulting π-electron macromolecules. This design strategy differs greatly from two other widely employed ones that introduce backbone spacers or linker atoms, and therefore offers a new motif for polymer semiconductors intended for organic electronics. **BTzOR**-containing head-to-head polymers exhibit promising properties, such as high degrees of subunit coplanarity induced by attractive (thiazolyl)S···O(alkoxy) contacts and the absence of repulsive (thiophene)C−H···H−C(arene) interactions, low bandgaps, highly crystalline film microstructures, and, with the proper imide *N*-substituents, good solubilities. More importantly, the electron-deficient thiazole core can offset the electron-donating tendencies of alkoxy substituents, and therefore **BTzOR** is more electron neutral than the previously reported thiophene-based **BTOR**, and thus **BTzOR**-based polymers have more balanced HOMO energetics. Furthermore, because **BTzOR** units impose less steric hindrance with respect to neighboring monomers by eliminating nonbonding C−H···H−C interactions, **BTzOR** can tolerate neighboring counits having greater steric hindrance while maintaining significant backbone coplanarity and conjugation, as illustrated here by a phthalimide unit. All of the present **BTzOR**-based polymers show substantial hole mobilities of 0.06−0.25 $cm^2/(V\ s)$, reflecting the backbone coplanarity and crystallinity. By polymerizing with an electron-deficient comonomer, the **BTzOR**-phthalimide copolymer exhibits an average TFT hole mobility of 0.13 $cm^2/(V\ s)$, high current on−off ratios (10^5), and enhanced device ambient stability versus **BTOR**-phthalimide copolymer TFTs. The high degrees of conjugation, low bandgaps, high crystallinities, and efficient transport properties render **BTzOR**-based polymers promising for organic electronics. Furthermore, the synthetic route reported here should be adaptable to other bithiazole-based building blocks.

EXPERIMENTAL SECTION

Details of monomer and polymer characterization and raw materials suppliers can be found in the Supporting Information.

Monomer Synthesis. *2,4-Dichlorothiazole* ***1***.[78] A mixture of 2,4-thiazolidinedione (50.0 g, 0.427 mol), phosphorus oxychloride (460 g, 3.0 mol), and pyridine (74 g, 0.93 mol) was refluxed for 3 h. The reaction mixture was then reduced in volume by 1/2 by distilling the volatiles through a short column. The resulting dark slurry was poured into ice (500 g). The mixture was then extracted with diethyl ether (3 × 500 mL), and the combined organic layer was washed successively with 5% aqueous NaOH (500 mL) and brine (500 mL). The separated organic layer was dried over $MgSO_4$, filtered, and concentrated in vacuo to a brown oil, which was purified by vacuum distillation through an air condenser. The solid distillate was recrystallized from 100 mL of cold hexanes to give 2,4-dichlorothiazole **1** as colorless needles (34 g, 52% yield). mp 42−43 °C (lit. 42−43 °C). ^{1}H NMR (500 MHz, $CDCl_3$, ppm): δ 7.04 (s, 1H).

4-Dichlorothiazole ***2***.[78] A mixture of 2,4-dichlorothiazole **1** (29 g, 188 mmol), zinc dust (43.5 g, 665 mmol), and acetic acid (400 mL) was refluxed for 6 h. After TLC indicated complete consumption of **1**, the mixture was cooled to room temperature and filtered. The filter cake was washed with acetic acid (3 × 30 mL). The filtrate was then poured into ice (1000 g) and was treated with about 50% (w/v) aqueous NaOH (0.65 L) until a slightly alkaline mixture resulted (pH = 9). The mixture was extracted with diethyl ether (3 × 300 mL), and the combined ethereal extracts were washed successively with saturated aqueous $NaHCO_3$ (300 mL) and brine (300 mL). The separated organic layer was dried over K_2CO_3, filtered, and concentrated in vacuo to give 4-chlorothiazole as a colorless liquid (16.5 g, 73% yield), which was pure enough for the next step without further purification. ^{1}H NMR (500 MHz, $CDCl_3$, ppm): δ 8.77 (d, 1H), 7.19 (d, 1H).

4-Methoxythiazole ***3***. A mixture of sodium methoxide, prepared by treating methanol (450 mL) with sodium metal (21 g, 913 mmol), and 4-chlorothiazole **2** (29.3 g, 245 mmol) was refluxed for 24 h. The mixture was next cooled to room temperature and was reduced in volume by about 1/2 by concentrating on a rotovap. The mixture was then dissolved in water (500 mL) and extracted with diethyl ether (3 × 300 mL). The combined ethereal extracts were washed with brine (500 mL), dried over $MgSO_4$, filtered, and concentrated in vacuo. The resulting red oil was purified by column chromatography using chloroform as the eluent, and then by vacuum distillation to give the title compound **3** as a colorless liquid (17.5 g, 62%). ^{1}H NMR (500 MHz, $CDCl_3$, ppm): δ 8.54 (d, 1H), 6.13 (d, 1H), 3.92 (s, 3H). ^{13}C NMR (125 MHz, $CDCl_3$, ppm): δ 166.25, 150.63, 88.85, 57.49.

4-Dodecoxythiazole ***4***. A mixture of 4-methoxythiazole **3** (4.0 g, 34.7 mmol), *n*-dodecanol (12.8 g, 68.7 mmol), *p*-toluenesulfonic acid monohydrate (0.7 g, 3.7 mmol), and toluene (75 mL) was heated at 130 °C for 24 h. The mixture was cooled to room temperature and purified by column chromatography using dichloromethane as the eluent. The resulting oily solid was recrystallized from cold pentane (20 mL) to give the product **4** as a colorless solid (5.15 g, 55%). ^{1}H NMR (500 MHz, $CDCl_3$, ppm): δ 8.52 (d, 1H), 6.09 (d, 1H), 4.09 (t, 2H), 1.79 (m, 2H), 1.45 (m, 2H), 1.25 (m, 16H), 0.87 (t, 3H). ^{13}C NMR (125 MHz, $CDCl_3$, ppm): δ 165.63, 150.28, 89.07, 70.47, 32.07, 29.81, 29.79, 29.74, 29.71, 29.51, 29.35, 26.10, 22.84, 14.33 (note: some peaks in the ^{13}C NMR spectrum overlap).

2-Triisopropylsilyl-4-dodecoxythiazole ***5***. A solution of 4-dodecoxythiazole **4** (4.38 g, 16.3 mmol) in THF (150 mL) was cooled to −78 °C. The resulting suspension was treated dropwise with *n*-BuLi (2.5 M in hexane, 6.50 mL, 16.3 mmol). The mixture was stirred for 2 h, and then the dry ice bath was removed for several minutes and a yellow solution resulted. The mixture was then cooled to −78 °C and treated with triisopropylchlorosilane (3.76 g, 19.5 mmol). The dry ice bath was removed, and the mixture was stirred at ambient temperature for 90 min. The mixture was next concentrated in vacuo and purified by

column chromatography using chloroform as the eluent to give the title compound as a pale yellow oil (6.24 g, 90% yield). ^{1}H NMR (500 MHz, $CDCl_3$, ppm): δ 6.24 (s, 1H), 4.12 (t, 2H), 1.83 (m, 2H), 1.45 (m, 5H), 1.23 (d, 16H), 1.32 (d, 18H), 0.89 (t, 3H). ^{13}C NMR (125 MHz, $CDCl_3$, ppm): δ 167.74, 167.37, 91.82, 70.65, 32.14, 29.88, 29.82, 29.79, 29.64, 29.57, 29.49, 26.25, 22.91, 18.70, 17.89, 14.34, 11.71 (note: some peaks in the ^{13}C NMR spectrum overlap).

2,2′-Bis(triisopropylsilyl)-4,4′-bis(dodecoxy)-5,5′-bithiazole ***6***. A solution of 2-triisopropylsilyl-4-dodecoxythiazole **5** (6.24 g, 14.7 mmol) in THF (150 mL) was cooled to −78 °C and treated dropwise with *n*-BuLi (2.5 M in hexanes; 6.45 mL, 16.1 mmol). After the mixture was stirred for 45 min, the dry ice bath was removed, and the mixture was stirred at ambient temperature for 1 h. The mixture was then cooled to 0 °C and treated with $Fe(acac)_3$ (5.69 g, 16.1 mmol). The reaction mixture was heated in an 80 °C oil bath for 2 h, cooled to room temperature, and filtered. The filter cake was washed with THF (3 × 25 mL). The filtrate was concentrated in vacuo and purified by column chromatography using dichloromethane/hexane (1:2) as eluent to give the title compound as a yellow solid (6.0 g, 96% yield). ^{1}H NMR (500 MHz, $CDCl_3$, ppm): δ 4.52 (t, 4H), 1.85 (m, 4H), 1.57 (m, 4H), 1.43 (m, 10H), 1.28 (m, 28H), 1.17 (d, 36H), 0.90 (t, 6H). ^{13}C NMR (125 MHz, $CDCl_3$, ppm): δ 162.18, 161.86, 105.94, 70.82, 32.17, 29.98, 29.96, 29.93, 29.90, 29.79, 29.63, 26.55, 22.94, 18.77, 14.35, 11.84 (note: some peaks in the ^{13}C NMR spectrum overlap).

4,4′-Bis(dodecoxy)-5,5′-bithiazole ***7***. To a solution of 2,2′-bis(triisopropylsilyl)-4,4′-bis(dodecoxy)-2,2′-bithiazole **6** (6.00 g, 7.06 mmol) in THF (150 mL) at 0 °C was added tetrabutylammonium fluoride (1.0 M in THF; 21.2 mL, 21.2 mmol) dropwise over 5 min. The mixture was next stirred for 30 min at 0 °C, and then the ice bath was removed and the mixture was stirred at 25 °C for 90 min. The mixture was treated with water (2 mL), concentrated in vacuo, and purified by column chromatography using dichloromethane/hexane (1:1) as the eluent. The product was further purified by recrystallization from hexane to give a yellow solid as the title compound (2.98 g, 79%). ^{1}H NMR (500 MHz, $CDCl_3$, ppm): δ 8.40 (s, 2H), 4.45 (t, 4H), 1.85 (m, 4H), 1.50 (m, 4H), 1.26 (m, 32H), 0.88 (t, 6H). ^{13}C NMR (125 MHz, $CDCl_3$, ppm): δ 159.52, 146.98, 102.93, 71.16, 32.14, 29.88, 29.82, 29.80, 29.78, 29.58, 29.54, 26.22, 22.91, 14.34 (note: some peaks in the ^{13}C NMR spectrum overlap).

2,2′-Dibromo-4,4′-bis(dodecoxy)-5,5′-bithiazole ***8***. A mixture of **7** (0.30 g, 0.56 mmol), *N*-bromosuccinimide (0.24 g, 1.35 mmol), and chloroform (40 mL) was heated in an oil bath at 60 °C for 1.5 h. The mixture was then concentrated in vacuo, and the resulting solid was purified by column chromatography using dichloromethane/hexane (1:1) as the eluent to afford colorless crystals as the product (0.286 g, 74%). mp 65 °C. ^{1}H NMR (500 MHz, $CDCl_3$, ppm): 4.38 (t, 4H), 1.80 (m, 4H), 1.47 (m, 4H), 1.34 (m, 32H), 0.89 (t, 6H). ^{13}C NMR (125 MHz, $CDCl_3$, ppm): δ 156.65, 131.45, 105.79, 71.82, 32.14, 29.89, 29.87, 29.80, 29.75, 29.59, 29.58, 29.45, 26.07, 22.92, 14.34. Anal. Calcd for $C_{30}H_{50}Br_2N_2O_2S_2$: C, 51.87; H, 7.25; N, 4.03. Found: C, 51.93; H, 7.44; N, 4.09.

2,2′-Bis(trimethylstannyl)-4,4′-bis(dodecoxy)-5,5′-bithiazole ***9***. A solution of **7** (0.373 g, 0.694 mmol) in THF (50 mL) was cooled to −78 °C. The resulting suspension was treated dropwise with *n*-BuLi (2.5 M in hexanes; 0.69 mL, 1.74 mmol) and stirred for 30 min. The dry ice bath was removed, and the mixture was stirred at ambient temperature for 30 min. The mixture was treated with 0.167 g (0.84 mmol) of trimethyltin chloride (1 M in hexane; 2.08 mL, 2.08 mmol) as one portion and heated in an oil bath at 60 °C for 1 h. The reaction mixture was then carefully quenched with H_2O and diluted with H_2O (100 mL). The reaction mixture was extracted with EtOAc (3 × 50 mL). The combined organic layer was washed with H_2O (100 mL), brine (100 mL), and dried over $MgSO_4$. After filtration and removal of solvent, the title compound was obtained as an off-white solid (587 mg, 98%). ^{1}H NMR (500 MHz, $CDCl_3$, ppm): 4.48 (t, 4H), 1.84 (m, 4H), 1.52 (m, 4H), 1.27 (m, 32H), 0.89 (t, 6H), 0.45 (s, 18H). ^{13}C NMR (125 MHz, $CDCl_3$, ppm): δ 167.35, 162.20, 106.54, 71.08, 32.15, 29.97, 29.94, 29.89, 29.88, 29.68, 29.60, 26.38, 22.92, 14.34, −7.90 (note: some peaks in the ^{13}C NMR spectrum overlap). Anal. Calcd for $C_{36}H_{68}N_2O_2S_2Sn_2$: C, 50.13; H, 7.95; N, 3.25. Found: C, 50.46; H, 7.72; N, 3.43.

5,5′-Dibromo-3,3′-bis(dodecoxy)-2,2′-bithiophene ***10***. To a solution of 3,3′-bis(dodecoxy)-2,2′-bithiophene[48] (0.32 g, 0.60 mmol) in chloroform (10 mL) was added *N*-bromosuccinimide (0.21 g, 1.20 mmol) in small portions over 2 min at −30 °C. After addition, the reaction was stirred at −30 °C for 2 h. The reaction then was warmed to 25 °C, and to the reaction was added 50 mL saturated aqueous Na_2SO_3 solution. The reaction was extracted three times with dichloromethane and the combined organic layer was washed with brine three times. After drying over $MgSO_4$ and filtration, the solvent was removed using rotovap, and a green residue was obtained as the crude product, which was purified by column chromatography using dichloromethane:hexane (1:1) as the eluent. The product was obtained as a yellow-green solid (0.38 g, 92%). ^{1}H NMR (500 MHz, $CDCl_3$, ppm): 6.82 (s, 2H), 4.04 (t, 4H), 1.83 (m, 4H), 1.48 (m, 4H), 1.31 (m, 32H), 0.89 (t, 6H). ^{13}C NMR (125 MHz, $CDCl_3$, ppm): δ 150.54, 119.25, 115.33, 110.05, 72.59, 32.15, 29.89, 29.86, 29.80, 29.76, 29.72, 29.59, 29.49, 26.14, 22.92, 14.35. Anal. Calcd for $C_{32}H_{52}Br_2O_2S_2$: C, 55.49; H, 7.57; N, 0.00. Found: C, 55.44; H, 7.38; N, not found.

5,5′-Bis(trimethylstannyl)-3,3′-bis(dodecoxy)-2,2′-bithiophene ***11***. A solution of 3,3′-bis(dodecoxy)-2,2′-bithiophene[48] (1.27 g, 2.37 mmol) in THF (60 mL) was cooled to −78 °C. The resulting suspension was treated dropwise with *n*-BuLi (2.5 M in hexanes; 2.10 mL, 5.22 mmol) and stirred for 30 min. The dry ice bath was removed, and the mixture was stirred at ambient temperature for 30 min. The mixture was treated with trimethyltin chloride (1 M in hexane; 5.93 mL, 5.93 mmol) as one portion. The reaction then was warmed to room temperature and stirred at 25 °C for 2 h. The reaction mixture was then carefully quenched with H_2O and diluted with H_2O (100 mL). The reaction mixture was extracted with EtOAc (3 × 50 mL), and the combined organic layer was washed with H_2O (100 mL), brine (100 mL), and dried over $MgSO_4$. After filtration and removal of solvent in vacuo, the title compound was obtained as an off-white solid, which was further purified by recrystallization from methanol to provide pale yellow needle-like crystals as the product (1.55 g, 76%). ^{1}H NMR (500 MHz, $CDCl_3$, ppm): 6.89 (s, 2H), 4.12 (t, 4H), 1.86 (m, 4H), 1.55 (m, 4H), 1.27 (m, 32H), 0.89 (t, 6H), 0.37 (s, 18H). ^{13}C NMR (125 MHz, $CDCl_3$, ppm): δ 154.03, 133.54, 123.78, 120.33, 72.16, 45.20, 32.15, 30.06, 29.93, 29.87, 29.74, 29.59, 26.45, 22.91, 14.34, −8.10 (note: some peaks in the ^{13}C NMR spectrum overlap). Anal. Calcd for $C_{38}H_{70}O_2S_2Sn_2$: C, 53.04; H, 8.20; N, 0.00. Found: C, 52.71; H, 7.91; N, not found.

Polymer Synthesis. *General Procedure for Stille Coupling Polymerizations in the Synthesis of* ***P1***−***P5***. An air-free flask was charged with the two monomers (0.20 mmol each), tris(dibenzylideneacetone)dipalladium(0) ($Pd_2(dba)_3$) and tris(*o*-tolyl)phosphine ($P(o\text{-tolyl})_3$) (1:8, $Pd_2(dba)_3$:$P(o\text{-tolyl})_3$ molar ratio; Pd loading 0.03−0.05 equiv). The flask and its contents were next subjected to three pump/purge cycles with argon, followed by addition of anhydrous toluene (8 mL) via syringe. The sealed reaction flask was then stirred at various temperatures for differing durations based on the solubility of the polymers. Next, 0.1 mL of 2-(tributylstanny)-thiophene was added, and the reaction mixture was stirred for another 12 h. Finally, 0.20 mL of 2-bromothiophene was added, and the reaction mixture was stirred for another 12 h. After cooling to room temperature, the deep-colored reaction mixture was slowly dripped into 100 mL of methanol (containing 5 mL of 12 N hydrochloric acid) with vigorous stirring. After stirring for 4 h, the solid precipitate was transferred to a Soxhlet thimble. After drying, the crude product was subjected to sequential Soxhlet extractions, with the choice of solvents and sequence depending on the solubility of the particular polymer. After final extraction with $CHCl_3$, the polymer solution was concentrated to approximately 20 mL, and then dripped into 100 mL of methanol with vigorous stirring. The polymer was collected by filtration and dried under reduced pressure to afford a deep colored solid as the product.

P1a. This polymer was synthesized from *N*-dodecyl-3,6-dibromophthalimide[48] and **9**. The polymerization was carried out at 60 °C for 2 h.

The solvent sequence for Soxhlet extraction was methanol, acetone, hexane, dichloromethane, and chloroform. This product was obtained as a blue solid (156 mg, 92% yield). M_n = 5.2 kDa, PDI = 3.2. ^{1}H NMR (400 MHz, $C_2D_2Cl_4$, 130 °C, ppm): δ 8.15 (br, 2H), 4.71 (br, 4H), 3.86 (br, 2H), 2.09 (br, 4H), 1.46 (m, 56H), 0.95 (br, 9H). Anal. Calcd for $C_{50}H_{77}N_3O_4S_2$: C, 70.79; H, 9.15; N, 4.95. Found: C, 71.23; H, 9.42; N, 4.77.

P1b. This polymer was synthesized from *N*-(2-ethylhexyl)-3,6-dibromophthalimide[48] and **9**. The polymerization was carried out at 110 °C for 48 h. The solvent sequence for Soxhlet extraction was methanol, acetone, hexane, dichloromethane, and chloroform. This product was obtained as a blue solid (135 mg, 85% yield). M_n = 34.6 kDa, PDI = 3.7. ^{1}H NMR (400 MHz, $C_2D_2Cl_4$, 130 °C, ppm): δ 8.17 (br, 2H), 4.71 (br, 4H), 3.79 (br, 2H), 2.07 (br, 4H), 1.99 (m, 1H), 1.49 (m, 44H), 0.97 (br, 12H). Anal. Calcd for $C_{46}H_{69}N_3O_4S_2$: C, 69.74; H, 8.78; N, 5.30. Found: C, 70.19; H, 8.47; N, 5.21.

P2. This polymer was synthesized from 4,4′-bis(*n*-dodecyl)-5,5′-bis(trimethylstannyl)-2,2′-bithiophene[87] and **8**. The polymerization was carried out at 110 °C for 72 h. The solvent sequence for Soxhlet extraction was methanol, acetone, hexane, and chloroform. This product was obtained as a blue solid (135 mg, 65% yield). M_n = 11.7 kDa, PDI = 2.0. ^{1}H NMR (400 MHz, $C_2D_2Cl_4$, 130 °C, ppm): δ 7.15 (s, 2H), 4.61 (br, 4H), 3.05 (br, 4H), 1.99 (br, 4H), 1.86 (br, 4H), 1.66 (br, 4H), 1.41 (m, 68H), 0.96 (b, 12H). Anal. Calcd for $C_{62}H_{102}N_2O_2S_4$: C, 71.90; H, 9.93; N, 2.70. Found: C, 72.18; H, 9.62; N, 3.01.

P3. This polymer was synthesized from **8** and **9**. The polymerization was carried out at 110 °C for 24 h. The solvent sequence for Soxhlet extraction was methanol, acetone, hexane, and chloroform. This product was obtained as a blue solid (184 mg, 86% yield). M_n = 8.8 kDa, PDI = 5.2. ^{1}H NMR (400 MHz, $C_2D_2Cl_4$, 130 °C, ppm): δ 4.65 (br, 4H), 1.99 (br, 4H), 1.47 (m, 36H), 0.96 (br, 6H). Anal. Calcd for $C_{30}H_{50}N_2O_2S_2$: C, 67.37; H, 9.42; N, 5.24. Found: C, 67.71; H, 9.69; N, 5.18.

P4a.[48] This polymer was synthesized from *N*-dodecyl-3,6-dibromophthalimide[48] and **11**. The polymerization was carried out at 50 °C for 2 h. The solvent sequence for Soxhlet extraction was methanol, acetone, hexane, and chloroform. This product was obtained as a blue solid (153 mg, 90% yield). M_n = 6.3 kDa, PDI = 3.6. ^{1}H NMR (400 MHz, $C_2D_2Cl_4$, 130 °C, ppm): δ 7.99 (brs, 2H), 7.91 (brs, 2H), 4.37 (brs, 4H), 3.79 (brs, 2H), 2.07 (brs, 4H), 1.77 (brs, 2H), 1.65 (brs, 4H), 1.42 (m, 50H), 0.91 (m, 9H). Anal. Calcd for $C_{52}H_{79}NO_4S_2$: C, 73.80; H, 9.41; N, 1.66. Found: C, 73.28; H, 9.23; N, 1.76.

P4b.[48] This polymer was synthesized from *N*-(2-ethylhexyl)-3,6-dibromophthalimide[48] and **11**. The polymerization was carried out at 110 °C for 48 h. The solvent sequence for Soxhlet extraction was methanol, acetone, hexane, dichloromethane, and chloroform. This product was obtained as a blue solid (137 mg, 87% yield). M_n = 44.3 kDa, PDI = 2.8. ^{1}H NMR (400 MHz, $C_2D_2Cl_4$, 130 °C, ppm): δ 7.89 (brs, 2H), 7.84 (brs, 2H), 4.32 (brs, 4H), 3.68 (brs, 2H), 2.00 (brs, 4H), 1.96 (m, 1H), 1.67 (brs, 4H), 1.34 (m, 40H), 0.95 (m, 12H). Anal. Calcd for $C_{48}H_{71}NO_4S_2$: C, 72.96; H, 9.06; N, 1.77. Found: C, 72.76; H, 9.11; N, 1.84.

P5. This polymer was synthesized from **10** and **11**. The polymerization was carried out at 110 °C for 24 h. The solvent sequence for Soxhlet extraction was methanol, acetone, hexane, and chloroform. This product was obtained as a blue solid (75 mg, 35% yield). M_n = 9.0 kDa, PDI = 4.2. ^{1}H NMR (400 MHz, $C_2D_2Cl_4$, 130 °C, ppm): δ 6.80 (brs, 2H), 4.12 (brs, 4H), 1.98 (m, 4H), 1.70 (m, 4H), 1.41 (brs, 32H), 0.96 (t, 6H). Anal. Calcd for $C_{32}H_{52}O_2S_2$: C, 72.12; H, 9.84; N, 0. Found: C, 71.66; H, 9.51; N, not found.

■ ASSOCIATED CONTENT

Supporting Information

Details of the monomer and polymer characterization and raw materials suppliers; procedure for TFT fabrication and characterization (XRD, AFM); and UV and DSC plots. This material is available free of charge via the Internet at http://pubs.acs.org.

■ AUTHOR INFORMATION

Corresponding Author

t-marks@northwestern.edu; a-facchetti@northwestern.edu

Notes

The authors declare no competing financial interest.

■ ACKNOWLEDGMENTS

We thank the ONR for financial support through the Multi-University Research Initiative (MURI Award N00014-11-1-0690) and AFOSR (FA9550-08-1-0331) for support of this research, and the NSF-MRSEC program through the Northwestern University Materials Research Science and Engineering Center for characterization facilities (DMR-1121262). R.P.O. acknowledges funding from the European Community's Seventh Framework Programme through a Marie Curie International Fellowship (Grant Agreement 234808).

■ REFERENCES

(1) McCulloch, I.; Ashraf, R. S.; Biniek, L.; Bronstein, H.; Combe, C.; Donaghey, J. E.; James, D. I.; Nielsen, C. B.; Schroeder, B. C.; Zhang, W. *Acc. Chem. Res.* **2012**, *45*, 714−722.

(2) Arias, A. C.; MacKenzie, J. D.; McCulloch, I.; Rivnay, J.; Salleo, A. *Chem. Rev.* **2010**, *110*, 3−24.

(3) Facchetti, A. *Chem. Mater.* **2011**, *23*, 733−758.

(4) Boudreault, P.-L. T.; Najari, A.; Leclerc, M. *Chem. Mater.* **2011**, *23*, 456−469.

(5) Sirringhaus, H. *Adv. Mater.* **2009**, *21*, 3859−3873.

(6) Osaka, I.; McCullough, R. D. *Acc. Chem. Res.* **2008**, *41*, 1202−1214.

(7) Henson, Z. B.; Müllen, K.; Bazan, G. C. *Nat. Chem.* **2012**, *4*, 699−704.

(8) Kim, F. S.; Ren, G.; Jenekhe, S. A. *Chem. Mater.* **2011**, *23*, 682−732.

(9) Osaka, I.; Shimawaki, M.; Mori, H.; Doi, I.; Miyazaki, E.; Koganezawa, T.; Takimiya, K. *J. Am. Chem. Soc.* **2012**, *134*, 3498−3507.

(10) Ko, S.; Hoke, E. T.; Pandey, L.; Hong, S. H.; Mondal, R.; Risko, C.; Yi, Y.; Noriega, R.; McGehee, M. D.; Brédas, J. L.; Salleo, A.; Bao, Z. *J. Am. Chem. Soc.* **2012**, *134*, 5222−5232.

(11) Yue, W.; Lv, A.; Gao, J.; Jiang, W.; Hao, L.; Li, C.; Li, Y.; Polander, L. E.; Barlow, S.; Hu, W.; Di Motta, S.; Negri, F.; Marder, S. R.; Wang, Z. *J. Am. Chem. Soc.* **2012**, *134*, 5770−5773.

(12) Wang, C.; Dong, H.; Hu, W.; Liu, Y.; Zhu, D. *Chem. Rev.* **2012**, *112*, 2208−2267.

(13) Wang, S.; Kiersnowski, A.; Pisula, W.; Müllen, K. *J. Am. Chem. Soc.* **2012**, *134*, 4015−4018.

(14) Guo, X.; Puniredd, S. R.; Baumgarten, M.; Pisula, W.; Müllen, K. *J. Am. Chem. Soc.* **2012**, *134*, 8404−8407.

(15) Yuen, J. D.; Fan, J.; Seifter, J.; Lim, B.; Hufschmid, R.; Heeger, A. J.; Wudl, F. *J. Am. Chem. Soc.* **2011**, *133*, 20799−20807.

(16) Chen, H.; Guo, Y.; Yu, G.; Zhao, Y.; Zhang, J.; Gao, D.; Liu, H.; Liu, Y. *Adv. Mater.* **2012**, *24*, 4618−4622.

(17) Mei, J.; Kim, D. H.; Ayzner, A. L.; Toney, M. F.; Bao, Z. *J. Am. Chem. Soc.* **2011**, *133*, 20130−20133.

(18) Lei, T.; Dou, J.-H.; Pei, J. *Adv. Mater.* **2012**, *24*, 6457−6461.

(19) McCullough, R. D.; Tristramnagle, S.; Williams, S. P.; Lowe, R. D.; Jayaraman, M. *J. Am. Chem. Soc.* **1993**, *115*, 4910−4911.

(20) Chen, T.-A.; Wu, X.; Rieke, R. D. *J. Am. Chem. Soc.* **1995**, *117*, 233−244.

(21) Sirringhaus, H.; Brown, P. J.; Friend, R. H.; Nielsen, M. M.; Bechgaard, K.; Langeveld-Voss, B. M. W.; Spiering, A. J. H.; Janssen, R. A. J.; Meijer, E. W.; Herwig, P.; de Leeuw, D. M. *Nature* **1999**, *401*, 685−688.

(22) Ong, B. S.; Wu, Y.; Liu, P.; Gardner, S. *J. Am. Chem. Soc.* **2004**, *126*, 3378−3379.
(23) McCulloch, I.; Heeney, M.; Bailey, C.; Genevicius, K.; MacDonald, I.; Shkunov, M.; Sparrowe, D.; Tierney, S.; Wagner, R.; Zhang, W.; Chabinyc, M. L.; Kline, R. J.; McGehee, M. D.; Toney, M. F. *Nat. Mater.* **2006**, *5*, 328−333.
(24) McCulloch, I.; Heeney, M.; Chabinyc, M. L.; DeLongchamp, D.; Kline, R. J.; Coelle, M.; Duffy, W.; Fischer, D.; Gundlach, D.; Hamadani, B.; Hamilton, R.; Richter, L.; Salleo, A.; Shkunov, M.; Sporrowe, D.; Tierney, S.; Zhang, W. *Adv. Mater.* **2009**, *21*, 1091−1109.
(25) Baklar, M.; Wobkenberg, P. H.; Sparrowe, D.; Goncalves, M.; McCulloch, I.; Heeney, M.; Anthopoulos, T.; Stingelin, N. *J. Mater. Chem.* **2010**, *20*, 1927−1931.
(26) Osaka, I.; Abe, T.; Shinamura, S.; Miyazaki, E.; Takimiya, K. *J. Am. Chem. Soc.* **2010**, *132*, 5000−5001.
(27) Heeney, M.; Bailey, C.; Genevicius, K.; Shkunov, M.; Sparrowe, D.; Tierney, S.; McCulloch, I. *J. Am. Chem. Soc.* **2005**, *127*, 1078−1079.
(28) Li, J.; Qin, F.; Li, C. M.; Bao, Q.; Chan-Park, M. B.; Zhang, W.; Qin, J.; Ong, B. S. *Chem. Mater.* **2008**, *20*, 2057−2059.
(29) Osaka, I.; Zhang, R.; Sauvé, G.; Smilgies, D.-M.; Kowalewski, T.; McCullough, R. D. *J. Am. Chem. Soc.* **2009**, *131*, 2521−2529.
(30) Ahmed, E.; Kim, F. S.; Xin, H.; Jenekhe, S. A. *Macromolecules* **2009**, *42*, 8615−8618.
(31) Usta, H.; Facchetti, A.; Marks, T. J. *J. Am. Chem. Soc.* **2008**, *130*, 8580−8581.
(32) Osaka, I.; Abe, T.; Shinamura, S.; Takimiya, K. *J. Am. Chem. Soc.* **2011**, *133*, 6852−6860.
(33) Asawapirom, U.; Scherf, U. *Macromol. Rapid Commun.* **2001**, *22*, 746−749.
(34) Zhang, M.; Tsao, H. N.; Pisula, W.; Yang, C. D.; Mishra, A. K.; Müllen, K. *J. Am. Chem. Soc.* **2007**, *129*, 3472−3473.
(35) Fei, Z.; Kim, Y.; Smith, J.; Domingo, E. B.; Stingelin, N.; McLachlan, M. A.; Song, K.; Anthopoulos, T. D.; Heeney, M. *Macromolecules* **2012**, *45*, 735−742.
(36) Amb, C. M.; Chen, S.; Graham, K. R.; Subbiah, J.; Small, C. E.; So, F.; Reynolds, J. R. *J. Am. Chem. Soc.* **2011**, *133*, 10062−10065.
(37) Beaujuge, P. M.; Pisula, W.; Tsao, H. N.; Ellinger, S.; Müllen, K.; Reynolds, J. R. *J. Am. Chem. Soc.* **2009**, *131*, 7514−7515.
(38) Liu, J.; Zhang, R.; Sauvé, G.; Kowalewski, T.; McCullough, R. D. *J. Am. Chem. Soc.* **2008**, *130*, 13167−13176.
(39) Chen, H.-Y.; Hou, J.; Hayden, A. E.; Yang, H.; Houk, K. N.; Yang, Y. *Adv. Mater.* **2010**, *22*, 371−375.
(40) Beaujuge, P. M.; Tsao, H. N.; Hansen, M. R.; Amb, C. M.; Risko, C.; Subbiah, J.; Choudhury, K. R.; Mavrinskiy, A.; Pisula, W.; Brédas, J. L.; So, F.; Müllen, K.; Reynolds, J. R. *J. Am. Chem. Soc.* **2012**, *134*, 8944−8957.
(41) Tsao, H. N.; Cho, D. M.; Park, I.; Hansen, M. R.; Mavrinskiy, A.; Yoon, D. Y.; Graf, R.; Pisula, W.; Spiess, H. W.; Müllen, K. *J. Am. Chem. Soc.* **2011**, *133*, 2605−2612.
(42) Tsao, H. N.; Cho, D.; Andreasen, J. W.; Rouhanipour, A.; Breiby, D. W.; Pisula, W.; Müllen, K. *Adv. Mater.* **2009**, *21*, 209−212.
(43) Tsao, H. N.; Müllen, K. *Chem. Soc. Rev.* **2010**, *39*, 2372−2386.
(44) Leenen, M. A. M.; Meyer, T.; Cucinotta, F.; Thiem, H.; Anselmann, R.; De Cola, L. *J. Polym. Sci., Part A: Polym. Chem.* **2010**, *48*, 1973−1978.
(45) Irvin, J. A.; Schwendeman, I.; Lee, Y.; Abboud, K. A.; Reynolds, J. R. *J. Polym. Sci., Part A: Polym. Chem.* **2001**, *39*, 2164−2178.
(46) Hergue, N.; Mallet, C.; Savitha, G.; Allain, M.; Frere, P.; Roncali, J. *Org. Lett.* **2011**, *13*, 1762−1765.
(47) Guo, X.; Watson, M. D. *Org. Lett.* **2008**, *10*, 5333−5336.
(48) Guo, X.; Kim, F. S.; Jenekhe, S. A.; Watson, M. D. *J. Am. Chem. Soc.* **2009**, *131*, 7206−7207.
(49) Kim, F. S.; Guo, X.; Watson, M. D.; Jenekhe, S. A. *Adv. Mater.* **2010**, *22*, 478−482.
(50) Usta, H.; Newman, C.; Chen, Z.; Facchetti, A. *Adv. Mater.* **2012**, *24*, 3678−3684.
(51) Berrouard, P.; Grenier, F.; Pouliot, J.-R.; Gagnon, E.; Tessier, C.; Leclerc, M. *Org. Lett.* **2011**, *13*, 38−41.
(52) Guo, X.; Xin, H.; Kim, F. S.; Liyanage, A. D. T.; Jenekhe, S. A.; Watson, M. D. *Macromolecules* **2011**, *44*, 269−277.
(53) Chu, T.-Y.; Lu, J.; Beaupre, S.; Zhang, Y.; Pouliot, J. R.; Wakim, S.; Zhou, J.; Leclerc, M.; Li, Z.; Ding, J.; Tao, Y. *J. Am. Chem. Soc.* **2011**, *133*, 4250−4253.
(54) Small, C. E.; Chen, S.; Subbiah, J.; Amb, C. M.; Tsang, S. W.; Lai, T. H.; Reynolds, J. R.; So, F. *Nat. Photonics* **2012**, *6*, 115−120.
(55) Guo, X.; Zhou, N.; Lou, S. J.; Hennek, J. W.; Ortiz, R. P.; Butler, M. R.; Boudreault, P.-L. T.; Strzalka, J.; Morin, P.-O.; Leclerc, M.; López Navarrete, J. T.; Ratner, M. A.; Chen, L. X.; Chang, R. P. H.; Facchetti, A.; Marks, T. J. *J. Am. Chem. Soc.* **2012**, *134*, 18427−18439.
(56) Pron, A.; Berrouard, P.; Leclerc, M. *Macromol. Chem. Phys.* **2013**, *214*, 7−16.
(57) Yamamoto, T.; Suganuma, H.; Maruyama, T.; Kubota, K. *J. Chem. Soc., Chem. Commun.* **1995**, 1613−1614.
(58) Yamamoto, T.; Suganuma, H.; Maruyama, T.; Inoue, T.; Muramatsu, Y.; Arai, M.; Komarudin, D.; Ooba, N.; Tomaru, S.; Sasaki, S.; Kubota, K. *Chem. Mater.* **1997**, *9*, 1217−1225.
(59) Politis, J. K.; Curtis, M. D.; Gonzalez, L.; Martin, D. C.; He, Y.; Kanicki, J. *Chem. Mater.* **1998**, *10*, 1713−1719.
(60) Osaka, I.; Zhang, R.; Liu, J.; Smilgies, D. M.; Kowalewski, T.; McCullough, R. D. *Chem. Mater.* **2010**, *22*, 4191−4196.
(61) Kim, D. H.; Lee, B.-L.; Moon, H.; Kang, H. M.; Jeong, E. J.; Park, J.-I.; Han, K.-M.; Lee, S.; Yoo, B. W.; Koo, B. W.; Kim, J. Y.; Lee, W. H.; Cho, K.; Becerril, H. A.; Bao, Z. *J. Am. Chem. Soc.* **2009**, *131*, 6124−6132.
(62) Ortiz, R. P.; Yan, H.; Facchetti, A.; Marks, T. J. *Materials* **2010**, *3*, 1533−1558.
(63) Li, Z.; Ding, J.; Song, N.; Lu, J.; Tao, Y. *J. Am. Chem. Soc.* **2010**, *132*, 13160−13161.
(64) Ying, L.; Hsu, B. B. Y.; Zhan, H.; Welch, G. C.; Zalar, P.; Perez, L. A.; Kramer, E. J.; Nguyen, T.-Q.; Heeger, A. J.; Wong, W.-Y.; Bazan, G. C. *J. Am. Chem. Soc.* **2011**, *133*, 18538−18541.
(65) Cho, H.-H.; Kang, T. E.; Kim, K.-H.; Kang, H.; Kim, H. J.; Kim, B. J. *Macromolecules* **2012**, *45*, 6415−6423.
(66) Yamamoto, T.; Kokubo, H.; Kobashi, M.; Sakai, Y. *Chem. Mater.* **2004**, *16*, 4616−4618.
(67) Balaban, A. T.; Oniciu, D. C.; Katritzky, A. R. *Chem. Rev.* **2004**, *104*, 2777−2812.
(68) Minkin, V. I.; Garnovskii, A. D.; Elguero, J.; Katritzky, A. R.; Denisko, O. V. *Adv. Heterocycl. Chem.* **2000**, *76*, 157−323.
(69) Kudla, C. J.; Dolfen, D.; Schottler, K. J.; Koenen, J.-M.; Breusov, D.; Allard, S.; Scherf, U. *Macromolecules* **2011**, *43*, 7864−7867.
(70) Nanos, J. I.; Kampf, J. W.; Curtis, M. D.; Gonzalez, L.; Martin, D. C. *Chem. Mater.* **1995**, *7*, 2232−2234.
(71) Politis, J. K.; Curtis, M. D.; González-Ronda, L.; Martin, D. C. *Chem. Mater.* **2000**, *12*, 2798−2804.
(72) Guo, X.; Ortiz, R. P.; Zheng, Y.; Hu, Y.; Noh, Y.-Y.; Baeg, K.-J.; Facchetti, A.; Marks, T. J. *J. Am. Chem. Soc.* **2011**, *133*, 1405−1418.
(73) Yamamoto, T.; Arai, M.; Kokubo, H.; Sasaki, S. *Macromolecules* **2003**, *36*, 7986−7993.
(74) Yamamoto, T.; Komarudin, D.; Arai, M.; Lee, B.-L.; Suganuma, H.; Asakawa, N.; Inoue, Y.; Kubota, K.; Sasaki, S.; Fukuda, T.; Matsuda, H. *J. Am. Chem. Soc.* **1998**, *120*, 2047−2058.
(75) Maruyama, T.; Suganuma, H.; Yamamoto, T. *Synth. Met.* **1995**, *74*, 183−185.
(76) Getmanenko, Y. A.; Risko, C.; Tongwa, P.; Kim, E.-G.; Li, H.; Sandhu, B.; Timofeeva, T.; Brédas, J.-L.; Marder, S. R. *J. Org. Chem.* **2011**, *76*, 2660−2671.
(77) Getmanenko, Y. A.; Tongwa, P.; Timofeeva, T. V.; Marder, S. R. *Org. Lett.* **2011**, *12*, 2136−2139.
(78) Reynaud, P.; Robba, M.; Moreau, R. C. *Bull. Soc. Chim. Fr.* **1962**, 1735.
(79) Stangeland, E. L.; Sammakia, T. *J. Org. Chem.* **2004**, *69*, 2381−2385.
(80) Pappenfus, T. M.; Mann, K. R. *Inorg. Chem.* **2001**, *40*, 6301−6307.

(81) Piliego, C.; Holcombe, T. W.; Douglas, J. D.; Woo, C. H.; Beaujuge, P. M.; Fréchet, J. M. J. *J. Am. Chem. Soc.* **2010**, *132*, 7595−7597.
(82) Würthner, F.; Ahmed, S.; Thalacker, C.; Debaerdemaeker, T. *Chem.-Eur. J.* **2002**, *8*, 4742−4750.
(83) Chen, D.; Zhao, Y.; Zhong, C.; Gao, S.; Yu, G.; Liu, Y.; Qin, J. *J. Mater. Chem.* **2012**, *22*, 14639−14644.
(84) Dierschke, F.; Jacob, J.; Müllen, K. *Synth. Met.* **2006**, *156*, 433−443.
(85) Ko, S.; Verploegen, E.; Hong, S.; Mondal, R.; Hoke, E. T.; Toney, M. F.; McGehee, M. D.; Bao, Z. *J. Am. Chem. Soc.* **2011**, *133*, 16722−16725.
(86) Chen, Z.; Lemke, H.; Albert-Seifried, S.; Caironi, M.; Nielsen, M. M.; Heeney, M.; Zhang, W.; McCulloch, I.; Sirringhaus, H. *Adv. Mater.* **2010**, *22*, 2371−2375.
(87) Guo, X.; Ortiz, R. P.; Zheng, Y.; Kim, M.-G.; Zhang, S.; Hu, Y.; Lu, G.; Facchetti, A.; Marks, T. J. *J. Am. Chem. Soc.* **2011**, *133*, 13685−13697.
(88) Kline, R. J.; McGehee, M. D.; Kadnikova, E. N.; Liu, J. S.; Fréchet, J. M. J. *Adv. Mater.* **2003**, *15*, 1519−1522.
(89) Li, J.; Zhao, Y.; Tan, H. S.; Guo, Y. L.; Di, C. A.; Yu, G.; Liu, Y. Q.; Lin, M.; Lim, S. H.; Zhou, Y. H.; Su, H. B.; Ong, B. S. *Sci. Rep.* **2012**, *2*, 754.
(90) Chabinyc, M. L. *Polym. Rev.* **2008**, *48*, 463−492.
(91) Ito, Y.; Virkar, A. A.; Mannsfeld, S.; Oh, J. H.; Toney, M.; Locklin, J.; Bao, Z. *J. Am. Chem. Soc.* **2009**, *131*, 9396−9404.